The temporal profile of calcium transients in voltage clamped gastric myocytes from *Bufo marinus*

J. G. McGeown, R. M. Drummond *, J. G. McCarron † and F. S. Fay *‡

*School of Biomedical Science, Queen's University of Belfast, 97 Lisburn Road, Belfast BT9 7BL, UK, *Department of Physiology and Biomedical Imaging Group, University of Massachusetts Medical Centre, 373 Plantation Street, Worcester, MA 01605, USA and †Division of Neuroscience and Biomedical Systems, Institute of Biomedical and Life Sciences, West Medical Building, University of Glasgow, Glasgow G12 8QQ, UK*

1. Decay in intracellular calcium concentration ($[Ca^{2+}]_i$) was recorded following step depolarizations in voltage clamped gastric myocytes from *Bufo marinus*.

2. Depolarizations (300 ms) to +10 mV were followed by three phases of $[Ca^{2+}]_i$ decay with repolarization to both −110 and −50 mV. The decline was initially rapid (mean fractional decay rate = 81 ± 11 % s^{-1} at −110 mV), then slowed (decay rate = 14 ± 2 % s^{-1}) and finally accelerated again (decay rate = 24 ± 3 % s^{-1}; $n = 19$).

3. The initial phase of rapid decay became shorter as the length of the depolarizing pulse increased but was unaffected by changes in pulse voltage.

4. The delayed acceleration in $[Ca^{2+}]_i$ decay was no longer seen when the duration of the depolarizing pulses was reduced to 100 ms, but was clearly evident following 500 ms pulses. This phase was abolished when the depolarizing voltage was altered to minimize the rise in $[Ca^{2+}]_i$.

5. Ryanodine and caffeine had no effect on the temporal profile of $[Ca^{2+}]_i$ decay.

6. Removal of extracellular Na^+ decreased the decay rate during all three phases at −110 mV, but this effect was particularly marked for the initial rapid phase of decay, the rate of which was reduced by 75 %. A delayed increase in decay rate was still seen.

7. Inhibition of mitochondrial Ca^{2+} uptake with cyanide, carbonyl cyanide *p*-trifluoromethoxyphenylhydrazone or Ruthenium Red had no effect on the initial rate of $[Ca^{2+}]_i$ decay but blocked the delayed acceleration.

8. These results are discussed in terms of a model in which rapid influx of Ca^{2+} produces a high subsarcolemmal $[Ca^{2+}]$, favouring rapid Ca^{2+} removal by near-membrane mechanisms, particularly Na^+–Ca^{2+} exchange. Mitochondrial Ca^{2+} removal produces a delayed increase in $[Ca^{2+}]_i$ decay if the global $[Ca^{2+}]_i$ is raised high enough for long enough.

Intracellular Ca^{2+} acts as a key element in signal transduction within smooth muscle (Somlyo, 1985). Changes in the cytoplasmic Ca^{2+} concentration ($[Ca^{2+}]_i$) depend on Ca^{2+} buffering within the cell and the balance between Ca^{2+} influx into the cytoplasm and Ca^{2+} removal from it. Considerable attention has been focused on both Ca^{2+} entry from the extracellular space via Ca^{2+} channels in the plasma membrane (Tsien & Tsien, 1990) and Ca^{2+} release from intracellular stores (Missiaen, Desmedt, Droogmans, Himpens & Casteels, 1992; Daniel, van Breemen, Schilling & Kwan, 1995). Processes contributing to Ca^{2+} decline have been less well investigated, despite their contribution both to the effective physiological buffering of the rise in $[Ca^{2+}]_i$ during stimulation and the rate of decay of $[Ca^{2+}]_i$ once stimulation has ceased. This decay rate will act as an important factor limiting the maximum rate of relaxation, since the rate of Ca^{2+} decline is much slower than the rate of membrane repolarization (Becker, Singer, Walsh & Fay, 1989). The behaviour of Ca^{2+} removal mechanisms is, therefore, likely to influence the duration of each contraction–relaxation cycle in spontaneously active, phasic smooth muscle. Consequently, it is important to have a clear description of the pattern of $[Ca^{2+}]_i$ change during the declining phase of the transient.

‡ To whom correspondence should be addressed.

One factor which may influence Ca^{2+} removal is the proposed existence of a limited diffusion space immediately adjacent to the plasma membrane (Chen, Cannell & van Breemen, 1992). Mathematical modelling suggests that the $[Ca^{2+}]$ achieved in such a subsarcolemmal space during rapid Ca^{2+} influx may be considerably higher than that in the bulk of the cytoplasm (Kargacin & Fay, 1991; Kargacin, 1994). This would help to explain why, when global Ca^{2+} indicators are used in intact cells, a number of near-membrane processes appear to be activated at lower (submicromolar) Ca^{2+} concentrations than would be expected from measurements of their Ca^{2+} sensitivities in isolated systems, which are typically in the 1–100 μM range (Morel & Godfraind, 1984; Singer & Walsh, 1987; Gurney, Tsien & Lester, 1987; Gunter & Pfeiffer, 1990; Carafoli, 1991). Recent experiments using simultaneous recordings from a single piece of tissue loaded with indicators of differing Ca^{2+} affinities add weight to the idea that there is an uneven distribution of Ca^{2+} within stimulated smooth muscle cells (Rembold, Van Riper & Chen, 1995). It has also been shown that Ca^{2+}-dependent K^+ currents rise and decay faster than the Ca^{2+} indicator signals recorded simultaneously in the same cell (Stehno-Bittel & Sturek, 1992; Ganitkevich & Isenberg, 1996) and this is taken to indicate that the subsarcolemmal $[Ca^{2+}]$ is changing more rapidly than the concentration in the bulk cytoplasm. Further evidence for such intracellular $[Ca^{2+}]$ gradients has come from newly developed membrane-associated Ca^{2+} indicators which have also revealed subsarcolemmal $[Ca^{2+}]$ transients which rise faster and reach greater peak values than those measured under identical conditions using fura-2 (Etter, Kuhn & Fay, 1994; Etter, Minta, Poenie & Fay, 1996).

It is possible that the existence of a subsarcolemmal space with restricted Ca^{2+} diffusion may facilitate calcium removal, either into the superficial sarcoplasmic reticulum (van Breemen & Saida, 1989; Chen *et al.* 1992) or by efflux across the plasma membrane (Scheid & Fay, 1984). By retaining Ca^{2+} close to peripherally located removal mechanisms, such a space may increase the rate of $[Ca^{2+}]_i$ decline as compared with situations in which the same Ca^{2+} load is distributed homogeneously throughout the cytoplasm. This is particularly likely if high subsarcolemmal concentrations allow the recruitment of low-affinity but high-capacity removal mechanisms such as Na^+–Ca^{2+} exchange (Morel & Godfraind, 1984; McCarron, Walsh & Fay, 1994). One way to examine this idea is to study Ca^{2+} decay whilst varying the duration of a depolarizing stimulus under voltage clamp conditions. The inward Ca^{2+} current is initially large, favouring accumulation of Ca^{2+} within any subsarcolemmal space, but as the pulse duration is prolonged the rate of influx rapidly declines due to inactivation of the current (Walsh & Singer, 1987). Diffusion should redistribute the Ca^{2+} load away from the plasma membrane, producing a more homogeneous pattern of $[Ca^{2+}]$ within the cell during longer pulses (Etter *et al.* 1996). In the present experiments, therefore, a combination of voltage clamp and microfluorimetry techniques (Yagi, Becker & Fay, 1988) were used to carry out a systematic examination of the effects of changes in the stimulus duration and strength on the temporal profile of $[Ca^{2+}]_i$ decline. This revealed a complexity not previously described, with multiphasic $[Ca^{2+}]_i$ decay, the number of phases seen being dependent on both stimulus duration and peak $[Ca^{2+}]_i$ achieved. Further experiments were carried out to examine the removal mechanisms involved in each phase. The findings are discussed both in terms of the possible influence of a subsarcolemmal space on near-membrane removal processes, as postulated above, and in relation to a delayed but $[Ca^{2+}]_i$-dependent upregulation of Ca^{2+} removal by mitochondria.

Preliminary aspects of this work have been communicated to The Physiological Society (McGeown & Fay, 1995) and the Royal Academy of Medicine in Ireland (McGeown, McCarron, Drummond & Fay, 1996).

METHODS

Toads (*Bufo marinus*) were killed by decapitation, as approved by the Unversity of Massachusetts Medical School Animal Care and Use Committee following guidelines of the USA Departments of Agriculture, and Health and Human Services. Myocytes, isolated from the stomach using standard techniques (Fay, Hoffman, Leclair & Merriam, 1982), were studied within 8 h under tight seal, whole-cell voltage clamp conditions with an Axoclamp-2A amplifier (Axon Instruments) in the single electrode voltage clamp mode. Fura-2 was loaded by diffusion from borosilicate patch electrodes (resistance, 4–8 MΩ) and dye-loaded cells were alternately excited at 340 and 380 nm. The ratio of the emitted fluorescence (recorded at 510 nm and corrected for background using recordings made with the pipette *in situ* but prior to rupturing the cell membrane) was recorded every 7 ms using a microfluorimeter (Yagi *et al.* 1988). This signal was converted to an intracellular Ca^{2+} concentration ($[Ca^{2+}]_i$) using the equation of Grynkiewicz, Poenie & Tsien (1985), with measured values of β (fluorescence ratio of equimolar dye, Ca^{2+}-free *vs.* Ca^{2+}-bound, exciting at 380 nm), R_{max} (fluorescence ratio exciting at 340 nm *vs.* 380 nm in the presence of saturating Ca^{2+}) and R_{min} (fluorescence ratio in the absence of Ca^{2+}), and a K_d of 200 nM, as experimentally determined *in vivo* for this cell type (Williams, Fogarty, Tsien & Fay, 1985). Experimental data were digitized and recorded on a PC for later analysis. Depolarizations were used to evoke an inward Ca^{2+} current (I_{Ca}) which rapidly raised $[Ca^{2+}]_i$. The return of $[Ca^{2+}]_i$ to resting levels was recorded following repolarization to the holding potential, which was −110 mV unless otherwise indicated. Use of a strongly negative holding potential ensures rapid deactivation of Ca^{2+} currents following repolarization and thus curtails initial slowing of Ca^{2+} decay by tail currents (Kostyuk & Shirokov, 1989). It also minimizes voltage-dependent inactivation so that Ca^{2+} influx during depolarization is maximal. Experiments were discarded if the holding current was variable since changes in the electrode seal resistance may lead to an influx of Ca^{2+} into the cell, artefactually slowing the declining phase of the transient.

The absolute rate of $[Ca^{2+}]_i$ decline ($-\Delta[Ca^{2+}]_i/\Delta t$) during single transients was calculated using a linear fit to data samples as previously described (Becker *et al.* 1989). A sliding, linear least-

squares fit was applied to either 51 or 101 data points, and the slope of the fitted line was determined. The negative of this gradient was then plotted at 50 or 100 ms intervals on the same time base as the transient.

All experiments were carried out at room temperature (24–26 °C) with the following solutions: bath solution (mM): NaCl, 94; KCl, 3; $CaCl_2$, 20; $MgCl_2$, 1; Hepes, 5; tetraethylammonium chloride, 10; pH adjusted to 7·4 with NaOH; pipette solution (mM): CsCl, 140; $MgCl_2$, 4; Na_2ATP, 3·5; fura-2 pentapotassium salt, 0·05; Pipes, 20; pH adjusted to 7·2 with CsOH. Intracellular caesium and extracellular tetraethylammonium block K^+ currents, allowing I_{Ca} to be isolated. Where required, Na^+-free solutions were prepared by replacing NaCl in the bath solution with LiCl and Na_2ATP in the pipette solution with MgATP. Reagents were obtained from the following sources: Na_2ATP, MgATP, Hepes, tetraethylammonium chloride, carbonyl cyanide *p*-trifluoromethoxyphenylhydrazone (FCCP; prepared as stock solution in DMSO) and caffeine from Sigma; ryanodine (prepared as stock solution in DMSO) and Pipes from Calbiochem (La Jolla, CA, USA); fura-2 pentapotassium from Molecular Probes (Eugene, OR, USA); NaCN from Aldrich (Milwaulkee, WI, USA).

Summarized data have been expressed in terms of the mean ± standard error of the mean (S.E.M.). The indicated number of observations included in each group of observations (n) is the number of cells tested. The number of different animals from which these were obtained is also noted. Visual inspection of the records of Ca^{2+} and the derived values for absolute decay rate allowed the $[Ca^{2+}]_i$ and time at the beginning and end of different phases of an individual transient (e.g. rapid or slow declining phases) to be identified. The data were then normalized by expressing the fall in $[Ca^{2+}]_i$ during each phase of the transient as a percentage of the total $[Ca^{2+}]_i$ change. This allowed results from cells with differing sizes of $[Ca^{2+}]_i$ transient, but similar transient shapes, to be combined. Normalized $[Ca^{2+}]_i$ changes were also used to calculate the rate of fall in percentage $[Ca^{2+}]_i$ (% s^{-1}) for each phase of the transient, and this will be referred to as the fractional decay rate. The statistical significance of apparent differences between mean percentage changes and fractional decay rates has been tested using the following non-parametric tests: (1) Wilcoxon signed rank test for comparison of paired observations involving transients recorded in the same cells under different conditions, e.g. following depolarizations of different duration; (2) Friedman test (two-way analysis of variance by ranks for matched samples) for comparisons of the three different phases identified within a single set of transients; (3) Mann–Whitney U test for comparisons between unpaired measurements from different groups of cells, e.g. those exposed to control and Na^+-free solutions. In addition, paired and unpaired t tests have been applied as relevant to mean absolute values for phase duration, peak $[Ca^{2+}]_i$ and peak I_{Ca} values. Differences between means were accepted as statistically significant at the 95% significance level.

RESULTS

Multiphasic calcium decline in voltage clamped cells

Under voltage clamp conditions, depolarization of isolated gastric myocytes to +10 mV elicited an inward Ca^{2+} current (Fig. 1*A*), producing a rapid rise in $[Ca^{2+}]_i$. On returning to the holding potential of −110 mV, $[Ca^{2+}]_i$ fell to resting levels. This decline was triphasic, as can be seen from a sample record for a single cell exposed to a depolarizing step of 200 ms duration (Fig. 1*B*, upper record). During the first 500 ms following repolarization Ca^{2+} levels declined rapidly (phase 1, Fig. 1*B* and *C*). This was followed by a more prolonged plateau phase lasting approximately 1·5 s during which the rate of $[Ca^{2+}]_i$ fall was considerably slowed (phase 2). Finally, $[Ca^{2+}]_i$ decline accelerated once more (phase 3). These three phases of $[Ca^{2+}]_i$ fall are also obvious when the absolute rate of $[Ca^{2+}]_i$ decline ($-\Delta[Ca^{2+}]_i/\Delta t$) is plotted on the same time base (Fig. 1*B*, lower graph). This has a peak-trough-peak pattern, as the rate of fall starts high, slows and then accelerates again.

Similar results were obtained using 300 ms depolarizations to +10 mV in a series of nineteen cells from fourteen different animals. Visual inspection of the transients allowed the $[Ca^{2+}]_i$ and time from repolarization to be determined for the beginning and end of each phase of $[Ca^{2+}]_i$ decay. The drop in $[Ca^{2+}]_i$ during each phase has been expressed as a percentage of the peak rise in $[Ca^{2+}]_i$ and the summarized data plotted (Fig. 2*A*). The changes in the rate of $[Ca^{2+}]_i$ decline can be seen more clearly when the rates of fall in percentage $[Ca^{2+}]_i$ during each phase (the fractional decay rates) are compared (Fig. 2*B*). The mean fractional decay rate decreased more than fivefold between phases 1 and 2, before increasing once more by over 70% during phase 3 ($P < 0{\cdot}0002$, Friedman test; $n = 19$).

In order to test whether multiphasic $[Ca^{2+}]_i$ decay was observed at potentials closer to those in the resting cell, a series of seven cells were depolarized for 300 ms as before but were then repolarized to −50 mV (Fig. 3). Both an initial rapid decline (mean decay rate of 78 ± 10% s^{-1}; phase 1 in Fig. 3*C*) and delayed acceleration in decay (from 10 ± 2% s^{-1} in phase 2 to 16 ± 2% s^{-1} in phase 3) were still seen ($P < 0{\cdot}005$, Friedman test; $n = 7$). In several cells, however, there was a continued rise in $[Ca^{2+}]_i$ after repolarization to −50 mV, perhaps due to continued Ca^{2+} influx prior to complete deactivation of the inward current. This was rarely seen following repolarization to −110 mV and therefore the more negative potential was used in all subsequent experiments.

Effects of stimulus duration on the temporal profile of transient decay

Previous studies with this preparation using longer depolarizing pulses (3 s) failed to reveal the multiphasic pattern of $[Ca^{2+}]_i$ decline seen in the current experiments (McCarron, McGeown, Reardon, Ikebe, Fay & Walsh, 1992). A protocol was devised, therefore, to test the possible dependence of the temporal profile of $[Ca^{2+}]_i$ decay on the test pulse duration. Pulses to +10 mV ranging in duration from 100 ms to 2 s were applied in random order. The resulting transients and the changes in the absolute rates of $[Ca^{2+}]_i$ decay have been plotted on the same time base for a single cell (Fig. 4). Triphasic decline in $[Ca^{2+}]_i$ is most clearly evident in pulses of intermediate duration. An initial, rapid phase of decline (phase 1 in Figs 1 and 2) was

the dominant feature following the shortest depolarization used, i.e. 100 ms. As the pulse duration was increased, e.g. to 200 or 300 ms, this early peak in $[Ca^{2+}]_i$ decay rate became attenuated while an intervening period of slower decline (phase 2 in Fig. 1) was followed by a secondary acceleration in the rate of $[Ca^{2+}]_i$ fall (phase 3 in Fig. 1). With even longer depolarizations (2 s), this complex pattern of $[Ca^{2+}]_i$ decay disappeared completely, leaving an essentially monophasic profile of decay. This seems to be equivalent to phase 3 in other records, phases 1 and 2 having ended before repolarization terminated Ca^{2+} influx.

A series of experiments similar to that described above was carried out on eight different cells (from 6 different animals) using randomly applied depolarizing steps of 100 ms, 500 ms and 1 s duration. The effect of changes in the duration of the depolarizing pulse on the profile of $[Ca^{2+}]_i$ decay has been summarized by normalizing each transient and recording $[Ca^{2+}]_i$ and time at the beginning and end of the phases seen. For each stimulus duration the mean percentage $[Ca^{2+}]_i$ decay during each of the three phases described above has been plotted against time elapsed since repolarization (Fig. 5*A*) and the decay rate during each

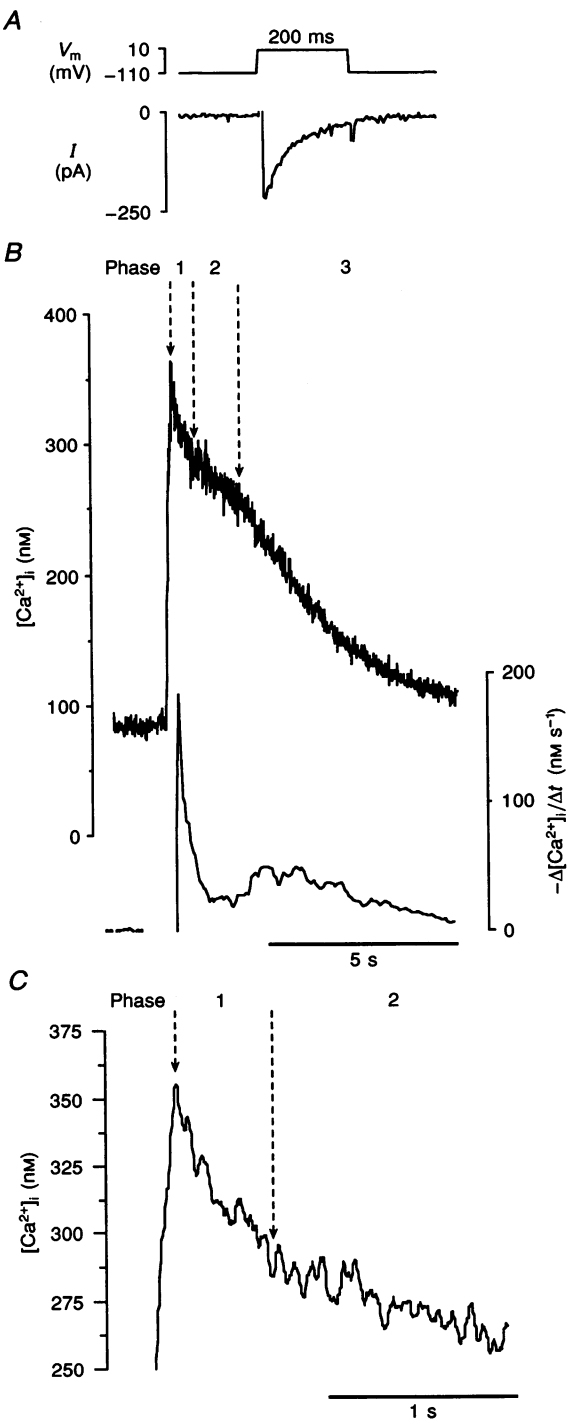

Figure 1. Triphasic $[Ca^{2+}]_i$ decay in a single transient

A, whole-cell current recording of inward current during a 200 ms step in membrane potential (V_m) from −110 to +10 mV. Capacitive transients have been blanked for clarity. *B*, $[Ca^{2+}]_i$ recorded simultaneously in the same cell (upper graph). Following repolarization, $[Ca^{2+}]_i$ decayed back to control levels in three phases (marked as 1, 2 and 3). These can be seen as an initial peak, followed by a trough and a secondary increase in a plot of the rate of decay of $[Ca^{2+}]_i$ against time for this transient ($-\Delta[Ca^{2+}]_i/\Delta t$; lower graph). *C*, same $[Ca^{2+}]_i$ data as in *B*, but plotted on a faster time base. (Data have been smoothed using an 11 point running average.)

phase of decline has been summarized (Fig. 5*B*). The mean fractional decay rate during the initial phase of rapid decline (phase 1) was similar following pulses of 100 and 500 ms. This phase lasted approximately twice as long after 100 ms pulses, however, and therefore accounted for twice as large a percentage drop in $[Ca^{2+}]_i$ (Fig. 5*A*; $P < 0{\cdot}05$, Wilcoxon signed rank test; $n = 8$). With a further increase in pulse length to 1 s, however, this early, rapid decay phase disappeared completely in all the cells studied ($n = 6$). The prominence of the second peak in decay rate (phase 3), on the other hand, increased with pulse duration. Following 100 ms pulses a clear acceleration was only observed in three of the eight cells tested, i.e. the slower phase 2 continued to the end of the transient in most cases. Thus, the mean fractional decay rate between the end of phase 1 and $[Ca^{2+}]_i$ values 30% below the peak ($15 \pm 3\%\ s^{-1}$) was almost identical to the subsequent rate of fall from 30 to 50% ($16 \pm 2\%\ s^{-1}$; $n = 8$) in these transients (Fig. 5). With pulses of 500 ms and 1 s duration, however, a clear acceleration (phase 3) was noted in every case, and the mean time and percentage fall in $[Ca^{2+}]_i$ at which this occurred has been plotted (Fig. 5*A*). Thus, for 500 ms pulses there was an increase in the mean fractional decay rate from $10 \pm 2\%\ s^{-1}$ during phase 2, to $21 \pm 1\%\ s^{-1}$ during phase 3 ($P < 0{\cdot}05$, Wilcoxon signed rank test; $n = 8$; Fig. 5*B*).

Effects of peak $[Ca^{2+}]_i$ on the temporal profile of transient decay

The shape of the $[Ca^{2+}]_i$ transient may be altered by the Ca^{2+} load presented during the depolarization pulse; indeed, this may account for some of the effects of changing pulse duration. In order to change total Ca^{2+} influx while keeping the pulse duration constant, depolarizing steps to different test potentials were applied. The pattern of $[Ca^{2+}]_i$ decay was analysed as before. Figure 6 shows records from one cell following 300 ms depolarizations to voltages of +10 mV, which produced a maximal rise in $[Ca^{2+}]_i$ in this cell, and to +30 mV, which produced a smaller inward current (Fig. 6*A*) and, therefore, a much smaller $[Ca^{2+}]_i$ rise (Fig. 6*B*). Plots of the absolute rate of $[Ca^{2+}]_i$ decline show that the pattern of decay is triphasic following the large transient but biphasic following the small transient. This contrast can be seen in Fig. 6*C* in which the same two $[Ca^{2+}]_i$ records have been scaled to allow comparison. Both records show an initial rapid decline although this is slightly smaller for the low-amplitude transient. The two transients then follow approximately parallel slopes up until about 1·8 s, after which decay accelerates in the case of the larger transient (+10 mV), with an increase in the negative slope from 9 to $15\%\ s^{-1}$. No such change is seen in the slope of the smaller transient (+30 mV).

Similar protocols confirmed this pattern in six cells (from 4 animals). In each cell, the voltage applied during the step depolarization was varied and the largest and smallest $[Ca^{2+}]_i$ transients obtained were compared. To avoid possible confusion due to time-dependent changes, the order in which the high and low peak $[Ca^{2+}]_i$ were elicited was randomized, with the smaller transient coming first in four out of seven cells. The mean peak inward currents producing the maximum and minimum transients seen were 359 ± 53 and 186 ± 39 pA, respectively ($P < 0{\cdot}05$, Wilcoxon signed

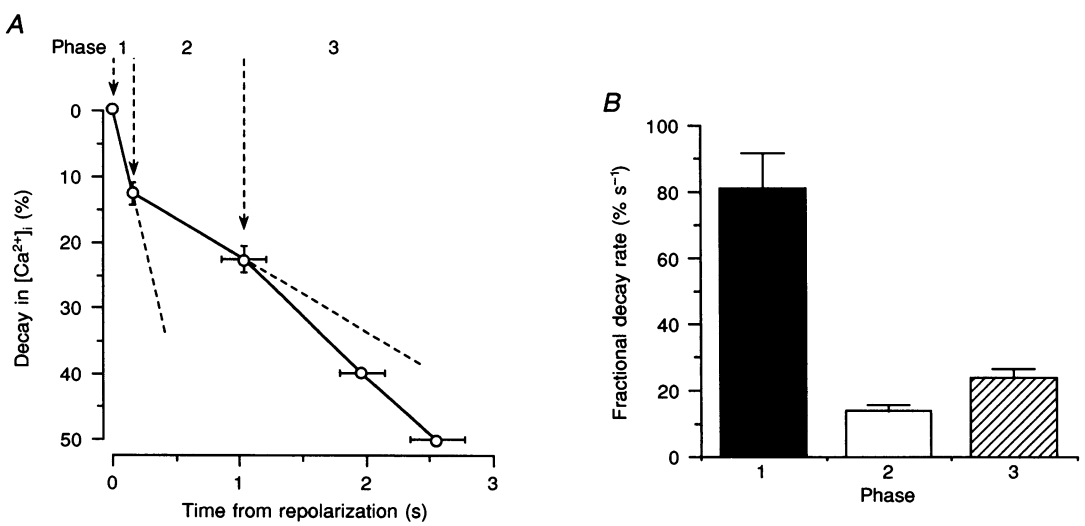

Figure 2. Summary data for the three phases of $[Ca^{2+}]_i$ decay

A, depolarizing pulses 300 ms long were applied to 19 cells (14 animals). The percentage decay in $[Ca^{2+}]_i$ (means ± S.E.M.) has been plotted against time for phases 1, 2 and 3 of decline, as identified by inspection of each transient (see Fig. 1). The mean time required for $[Ca^{2+}]_i$ to decay by 40 and 50% has also been plotted. Dashed extrapolations indicate the slopes during phases 1 and 2 for comparison. *B*, summary of the fractional decay rate for $[Ca^{2+}]_i$ (means ± S.E.M.) during each of the identified phases of decline. The rate for phase 3 was measured from the end of phase 2 to 50% decay in each case.

rank test) and these produced rises in $[Ca^{2+}]_i$ of 417 ± 140 and 140 ± 32 nM, respectively ($P < 0{\cdot}02$, Wilcoxon signed rank test; $n = 6$). Summarizing the data for the different phases of decay in each transient indicated that there were no statistically significant differences in the mean durations (data not shown) and fractional $[Ca^{2+}]_i$ decay rates during the initial fast phase of decline (phase 1) following transients of differing amplitudes (Fig. 6*D*). This phase accounted for a mean percentage decay of 14 ± 4 and 18 ± 5% for the largest and smallest transients, respectively (*P*, not significant; n.s.). In the case of the larger rises in $[Ca^{2+}]_i$ there was also a delayed, secondary increase in the mean fractional rate of $[Ca^{2+}]_i$ decay, which rose from 10 ± 2 to 29 ± 9% s^{-1} ($P < 0{\cdot}05$, Wilcoxon signed rank test; $n = 6$) between phases 2 and 3 (Fig. 6*D*). No such acceleration of decay was seen following small $[Ca^{2+}]_i$ increases, however, with a linear decline in percentage $[Ca^{2+}]_i$ at an average rate of 14 ± 2% s^{-1} from the end of phase 1 to 50% decay. These results suggest that the secondary increase in decay rate is only stimulated when $[Ca^{2+}]_i$ rises above a minimum threshold. The fact that this effect was observed regardless of whether the larger rise in $[Ca^{2+}]_i$ was evoked using a more positive (3 out of 7 cells) or less positive (4 out of 7 cells) depolarizing step than that producing the smaller $[Ca^{2+}]_i$ rise in a given cell is consistent with a dependence on the magnitude of the $[Ca^{2+}]_i$ rise, rather than the voltage applied during depolarization.

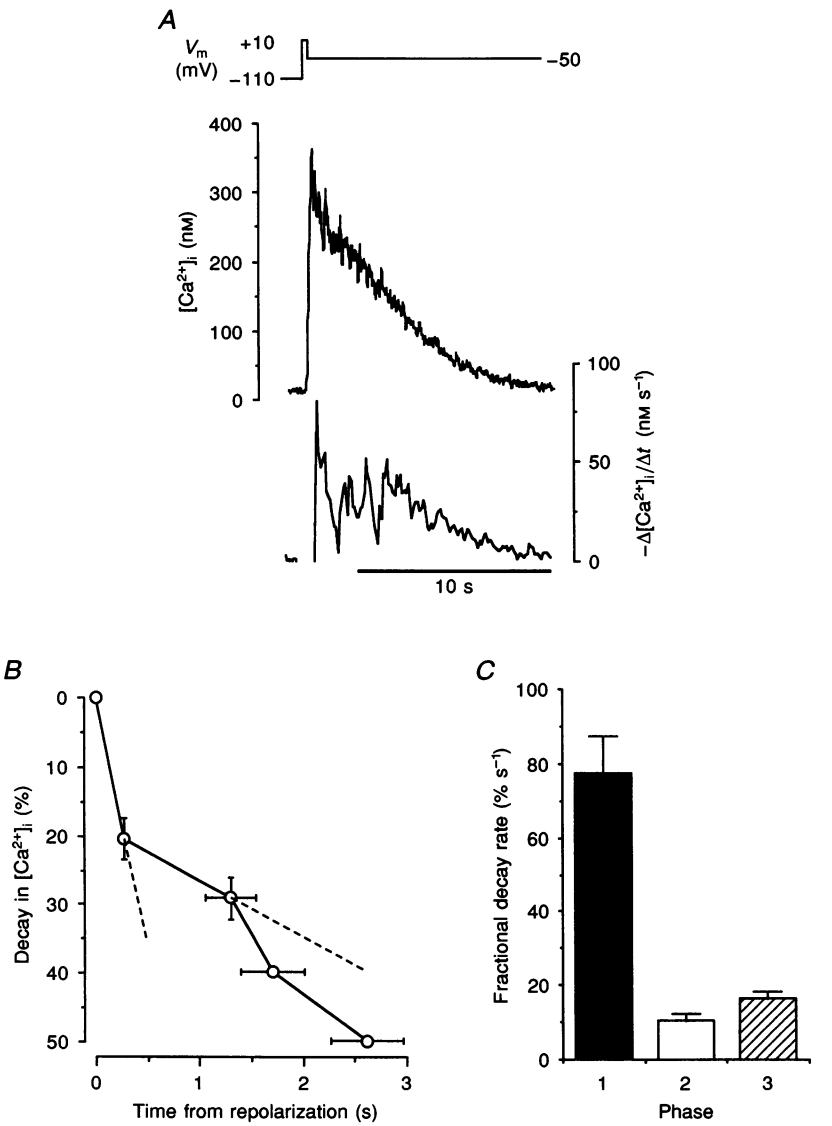

Figure 3. $[Ca^{2+}]_i$ decay following repolarization to −50 mV

A, $[Ca^{2+}]_i$ and $-\Delta[Ca^{2+}]_i/\Delta t$ for a single cell which was depolarized from −110 to +10 mV for 300 ms and then repolarized to −50 mV during the period of $[Ca^{2+}]_i$ decay (top panel). *B*, summarized data showing percentage decay in $[Ca^{2+}]_i$ against time (means ± S.E.M.) for 7 cells (1 animal) exposed to the protocol in *A*. Dashed extrapolations indicate slopes for comparison. *C*, mean fractional rates of $[Ca^{2+}]_i$ decay (± S.E.M.) during each phase of transient decline in these cells.

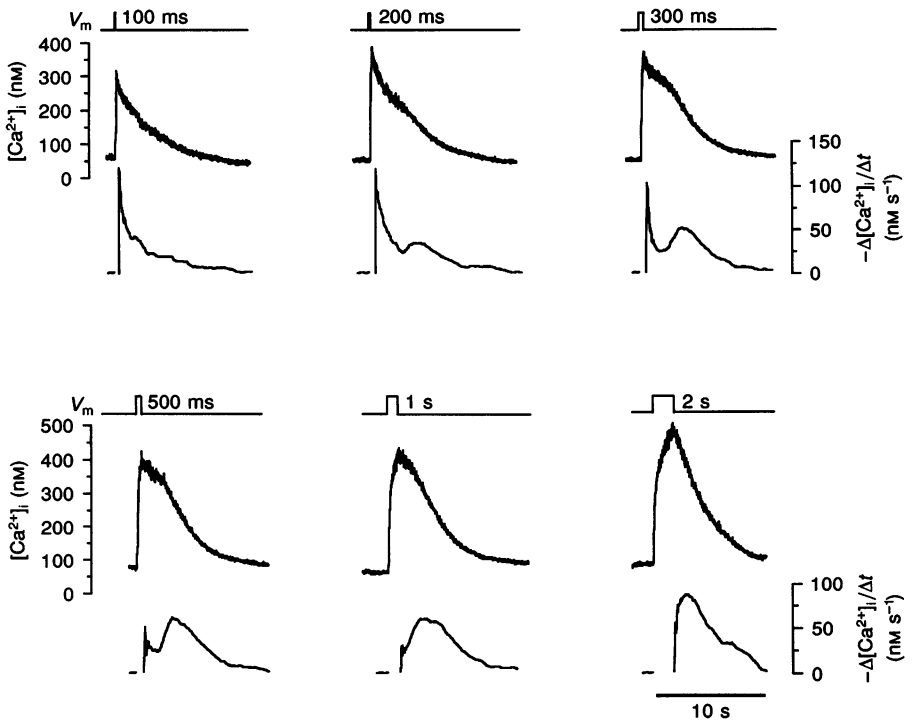

Figure 4. $[Ca^{2+}]_i$ decay following depolarizing pulses of varying duration

$[Ca^{2+}]_i$ recordings following +10 mV depolarizations of varying durations applied to a single cell. The absolute rate of calcium decline ($-\Delta[Ca^{2+}]_i/\Delta t$) has been plotted below each transient.

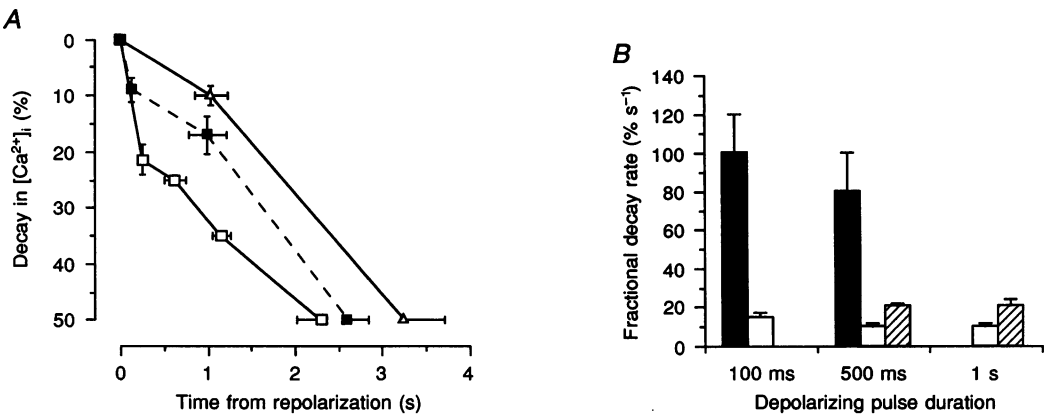

Figure 5. Summary of $[Ca^{2+}]_i$ decay following depolarizing pulses of 3 different durations

A, plot of mean percentage decay in $[Ca^{2+}]_i$ against time for 8 cells (6 different animals), each of which was depolarized to +10 mV for 100 ms, 500 ms and 1 s. For 500 ms pulses (■) the percentage decay in $[Ca^{2+}]_i$ (means ± S.E.M.) and time from repolarization (means ± S.E.M.) is plotted for phases 1, 2 and 3 (see Fig. 2), as is the time required for 50% decay. For 1 s pulses (△) phase 1 was not present and so only phases 2 and 3 are shown. In the case of 100 ms pulses (□) a transition from phase 2 to phase 3 was only seen in a minority of cells and so phase 1 values are plotted along with the mean time required for 25, 35 and 50% $[Ca^{2+}]_i$ decay. *B*, bar chart summarizing $[Ca^{2+}]_i$ fractional decay rates (means ± S.E.M.) during phases 1 (■), 2 (□) and 3 (▨) for the 3 depolarizing pulse durations used. For transients showing an appreciable delayed acceleration in decay (phase 3) the phase 2 fractional decay rate was measured from the end of phase 1 to the onset of phase 3 and the phase 3 rate was measured from the onset of phase 3 to 50% decay. In transients in which no such acceleration was seen, the fractional decay rate between the end of phase 1 and 50% decay was entered for phase 2. These conventions were used when similar calculations were being carried out for other protocols.

Temporal profile of $[Ca^{2+}]_i$ decay in the presence of ryanodine and caffeine

The rate of $[Ca^{2+}]_i$ decline at any time after a depolarizing pulse will depend on the balance between removal of free Ca^{2+} by chemical buffering, uptake into stores or extrusion across the plasma membrane, and Ca^{2+} influx across the cell membrane or release from intracellular stores. Ryanodine-sensitive Ca^{2+} stores may contribute to Ca^{2+} removal or give rise to Ca^{2+}-induced Ca^{2+} release. Either process might account for changing rates of $[Ca^{2+}]_i$ decay over time following depolarization. Exposure to ryanodine (100 μM in the bath for 40 min prior to the experiment), however, had little effect on the shape of $[Ca^{2+}]_i$ decline, as seen in records of $[Ca^{2+}]_i$ and $-\Delta[Ca^{2+}]_i/\Delta t$ from a single experiment using a 400 ms depolarization to +10 mV (Fig. 7*A*). This cell had been depolarized to +10 mV four times over the previous 2 min to allow use-dependent block by ryanodine to become fully established. In a series of similar experiments, six cells (from 3 animals) were exposed to ryanodine in both the bath solution (50 μM) and in the pipette solution (50 μM). Following rupture of the on-cell patch, 5 min were allowed to elapse prior to recording transients to permit diffusion of ryanodine throughout the cell. The amplitude of the $[Ca^{2+}]_i$ rise during depolarization was reduced in these cells, with a mean peak $[Ca^{2+}]_i$ of 302 ± 20 nM ($n = 6$), compared with 454 ± 47 nM in control cells ($n = 18$; $P < 0.05$, Mann–

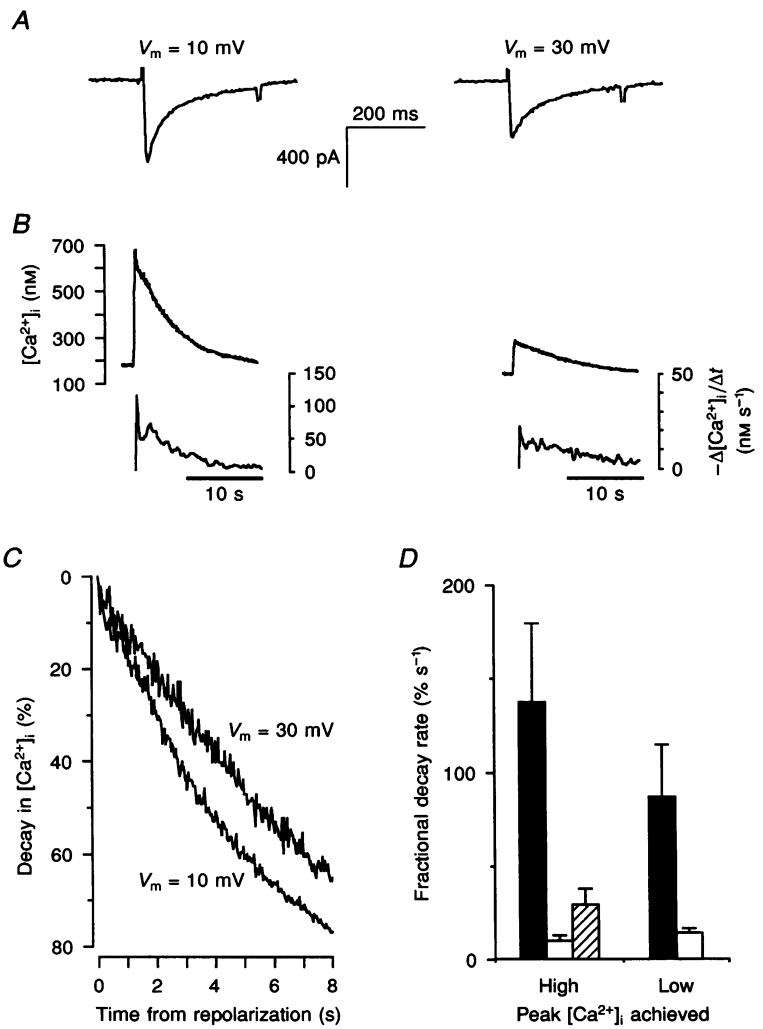

Figure 6. $[Ca^{2+}]_i$ decay following depolarizing pulses of varying amplitude

A, inward currents recorded during 300 ms depolarizing pulses to +10 mV (left) and +30 mV (right) in the same cell. *B*, changes in $[Ca^{2+}]_i$ and $-\Delta[Ca^{2+}]_i/\Delta t$ with time for the transients produced by these currents. *C*, percentage decay in $[Ca^{2+}]_i$ plotted against time for the same two transients as in *B*. Scaling of the smaller transient (+30 mV; upper graph) has increased signal noise relative to the larger transient (+10 mV; lower graph). *D*, summary of $[Ca^{2+}]_i$ fractional decay rates (means ± S.E.M.) for pairs of transients producing high (left-hand bars) and low (right-hand bars) peak Ca^{2+} levels in a series of 6 cells (4 animals). Small transients were not associated with a statistically significant delayed increase in rate and so only phases 1 and 2 (from the end of phase 1 to 50%) are plotted. ■, phase 1; □, phase 2; ▨, phase 3.

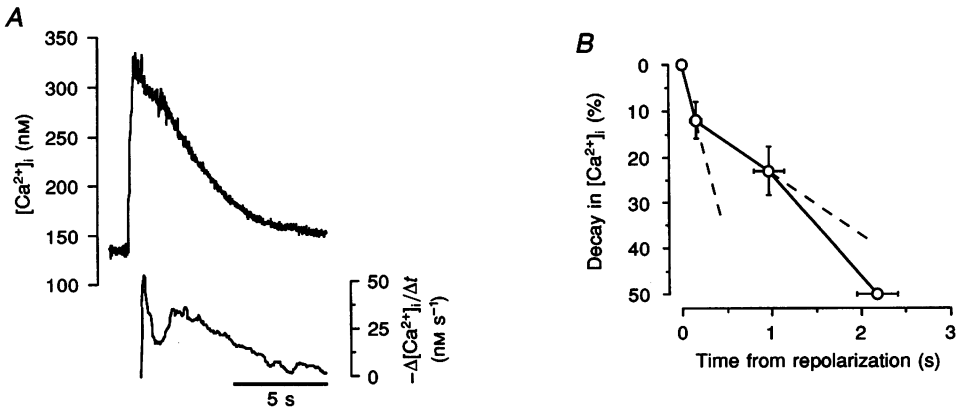

Figure 7. $[Ca^{2+}]_i$ decay in the presence of ryanodine

A, records showing $[Ca^{2+}]_i$ and $-\Delta[Ca^{2+}]_i/\Delta t$ for a single cell following a 400 ms depolarization to +10 mV in the presence of 100 μM ryanodine in the bath solution. *B*, summarized data for 6 cells (from 3 animals) showing percentage decay in $[Ca^{2+}]_i$ against time (means ± S.E.M.) following 300 ms step depolarizations in the presence of 50 μM ryanodine in both bath and pipette solutions.

Whitney *U* test). This may reflect a role for Ca^{2+}-induced Ca^{2+} release during the rising phase of the transient since the average ratio of $[Ca^{2+}]_i$ rise to peak inward current ($\Delta[Ca^{2+}]_i/I_{Ca}$) was reduced from 1·155 nM pA^{-1} in control cells ($n = 18$), to 0·483 nM pA^{-1} in the presence of ryanodine ($n = 6$; $P < 0{\cdot}01$, Mann–Whitney *U* test). Ryanodine did not change the temporal profile of $[Ca^{2+}]_i$ decay, however, with three phases similar to those seen following 300 ms depolarizing pulses under control conditions clearly evident (Fig. 7*B*). The mean fractional decay rates for each phase

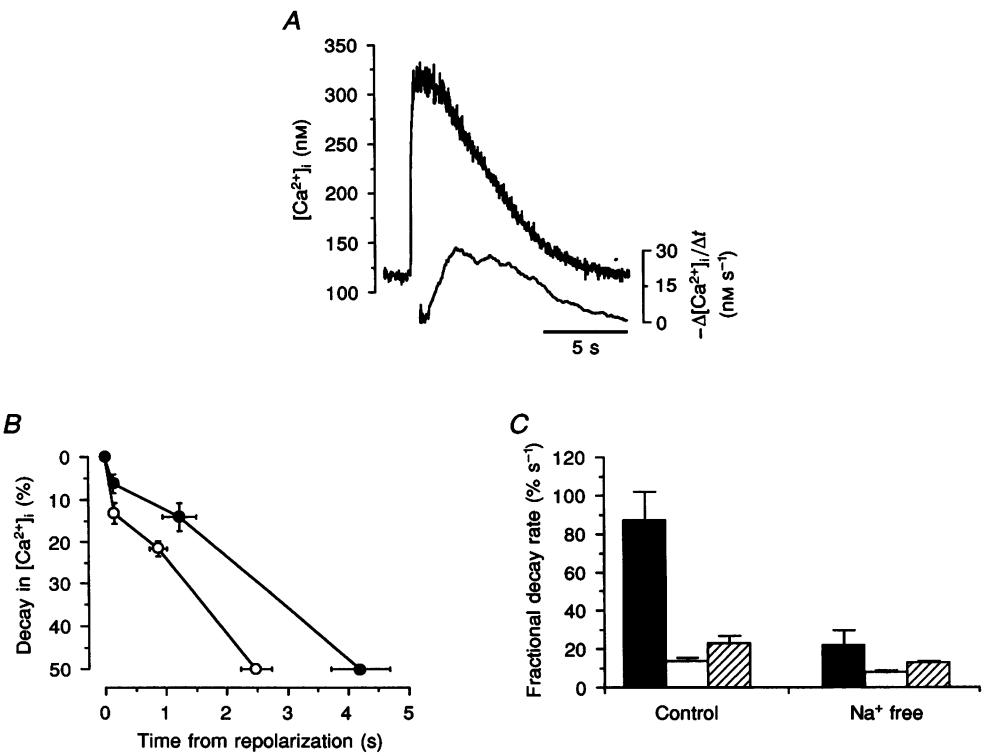

Figure 8. $[Ca^{2+}]_i$ decay in the absence of Na^+

A, $[Ca^{2+}]_i$ and $-\Delta[Ca^{2+}]_i/\Delta t$ records for a single cell following a 300 ms depolarization in Na^+-free solution (external Na^+ replaced with Li^+; Na_2ATP in the pipette solution replaced with MgATP). *B*, summarized data showing percentage decay in $[Ca^{2+}]_i$ against time (means ± S.E.M.) following 300 ms step depolarizations for 11 control cells (○) and 10 cells exposed to Na^+-free solution in both the bath and the pipette (●). *C*, mean fractional rates of $[Ca^{2+}]_i$ decay (± S.E.M.) during each identifiable phase of transient decline under control (left) and Na^+-free (right) conditions. ■, phase 1; □, phase 2; ▨, phase 3.

were 107 ± 46% s^{-1} during phase 1, falling to 15 ± 3% s^{-1} in phase 2 with a subsequent acceleration to 27 ± 4% s^{-1} in phase 3 ($P < 0.05$, Friedman test; $n = 6$). There were no statistically significant differences between the mean values of duration, total percentage fall in $[Ca^{2+}]_i$, or $[Ca^{2+}]_i$ fractional decay rates for any of the three phases in cells exposed to ryanodine compared with those in the previously described controls (n.s., Mann–Whitney U test). This suggests that Ca^{2+} uptake into, or release from, the ryanodine-sensitive Ca^{2+} store is not required for multiphasic $[Ca^{2+}]_i$ decline. Exposure to extracellular caffeine (10 mM), a well-recognized ryanodine receptor agonist, also failed to alter the temporal profile in three cells (data not shown).

Effect of Na^+ removal on temporal profile of $[Ca^{2+}]_i$ decay

Previous studies using toad gastric myocytes have demonstrated that Na^+–Ca^{2+} exchange contributes to the decline of $[Ca^{2+}]_i$ (McCarron *et al.* 1994). In order to determine what role Na^+–Ca^{2+} exchange played during the three phases of $[Ca^{2+}]_i$ decline, the Na^+ in the bath solution was replaced with Li^+ so that Ca^{2+} removal by Na^+–Ca^{2+} exchange was inhibited. The small amount of Na^+ normally present in the pipette solution as Na_2ATP was also replaced with MgATP in both Na^+-free and parallel control experiments in an attempt to limit or prevent possible Ca^{2+} influx by reverse exchange. Removal of external Na^+ slowed all three phases of $[Ca^{2+}]_i$ decay following a 300 ms depolarization (Fig. 8*C*) but appeared to have the most marked effect on phase 1, abolishing it completely in five out of ten cells. The $[Ca^{2+}]_i$ and $-\Delta[Ca^{2+}]_i/\Delta t$ records from one such cell have been plotted and demonstrate that $[Ca^{2+}]_i$ decay following repolarization was slow initially (Fig. 8*A*). In contrast, an initial rapid phase of decay was clearly visible in ten out of eleven control experiments carried out over the same time period in the presence of normal extracellular $[Na^+]$. Overall, the mean fractional rate of $[Ca^{2+}]_i$ decay during phase 1 was reduced by 75% in the absence of Na^+ ($P < 0.002$, Mann–Whitney U test; Fig. 8*C*). The rates of decay during phases 2 and 3 were also lower than those observed under control conditions, but a delayed acceleration of decay was

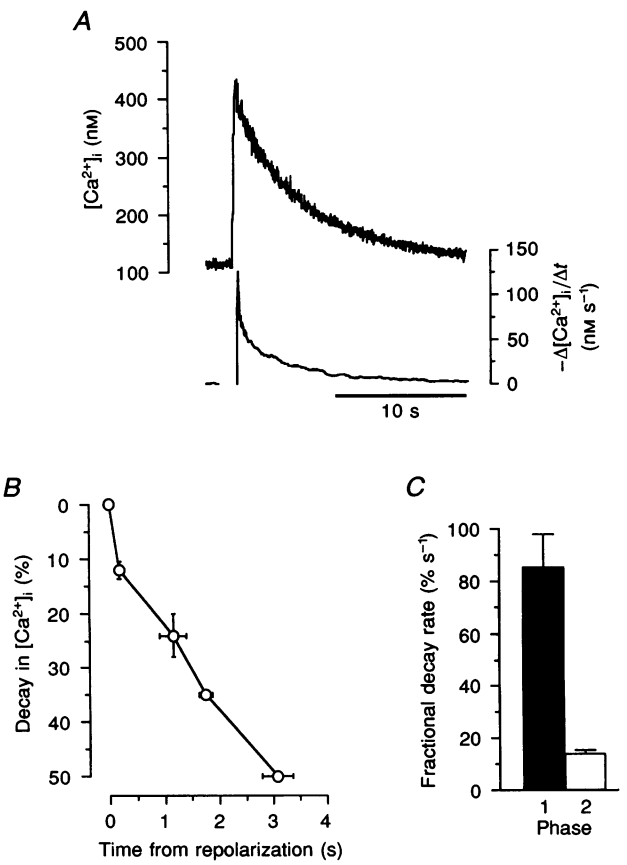

Figure 9. $[Ca^{2+}]_i$ decay in the presence of CN^-

A, $[Ca^{2+}]_i$ and $-\Delta[Ca^{2+}]_i/\Delta t$ records for a single cell exposed to 2 mM CN^- in the bath solution and depolarized to +10 mV for 300 ms. *B*, summarized data from 7 CN^--treated cells (3 animals). The mean percentage decay in $[Ca^{2+}]_i$ (± S.E.M.) is plotted against time. *C*, summary of the mean fractional rate of $[Ca^{2+}]_i$ decay (± S.E.M.) for the initial phase of rapid decline (phase 1) and from the end of phase 1 to 50% decay (phase 2).

still present in nine out of ten cells tested under Na^+-free conditions. This is seen very clearly as a rise in the absolute rate of $[Ca^{2+}]_i$ decay in the record shown (Fig. 8*A*), and is confirmed by the summarized data, with the mean fractional rate of decay increasing from 8 ± 1 to $13 \pm 1\%$ s^{-1} between phases 2 and 3, respectively ($n = 10$; $P < 0{\cdot}05$, Wilcoxon signed rank test; Fig. 8*C*).

Effect of mitochondrial inhibitors on temporal profile of $[Ca^{2+}]_i$ decay

Further experiments were carried out to determine whether mitochondrial Ca^{2+} uptake contributed to one or more of the phases of $[Ca^{2+}]_i$ decay seen following 300 ms depolarizing pulses. In the first protocol, cells were exposed to cyanide (CN^-) at a concentration of 2 mM in the bath solution. CN^- inhibits the final enzyme in the mitochondrial electron transport chain, i.e. cytochrome oxidase, thus blocking mitochondrial extrusion of protons. This results in mitochondrial depolarization which diminishes the electrochemical gradient driving mitochondrial Ca^{2+} uptake (for review see Gunter & Pfeiffer, 1990). Recent studies have demonstrated that CN^- both reduces the mitochondrial membrane potential and slows cytoplasmic $[Ca^{2+}]_i$ decay in isolated gastric myocytes from *Bufo marinus* (Drummond & Fay, 1996). In the current experiments, CN^- was also found to modify the temporal profile of decay in these cells by inhibiting the secondary acceleration (phase 3) of $[Ca^{2+}]_i$ decay normally seen under control conditions. This is well demonstrated by a single record obtained in the presence of CN^- (Fig. 9*A*), in which a brief period of rapid decline in $[Ca^{2+}]_i$ is followed by an apparently exponential fall towards baseline, with no secondary acceleration in decay. In a series of seven such experiments, the mean values for the duration, percentage fall in $[Ca^{2+}]_i$ and fractional rate of decay (Fig. 9*B* and *C*) for phase 1 were similar to those under control conditions (Fig. 2). The rate of decay then slowed, and although a slight secondary increase in the rate of $[Ca^{2+}]_i$ fall was seen in four out of seven cells, this was not statistically significant. Thus, mean percentage $[Ca^{2+}]_i$ decayed linearly from the end of phase 1 down to 50% of maximum (Fig. 9*B*).

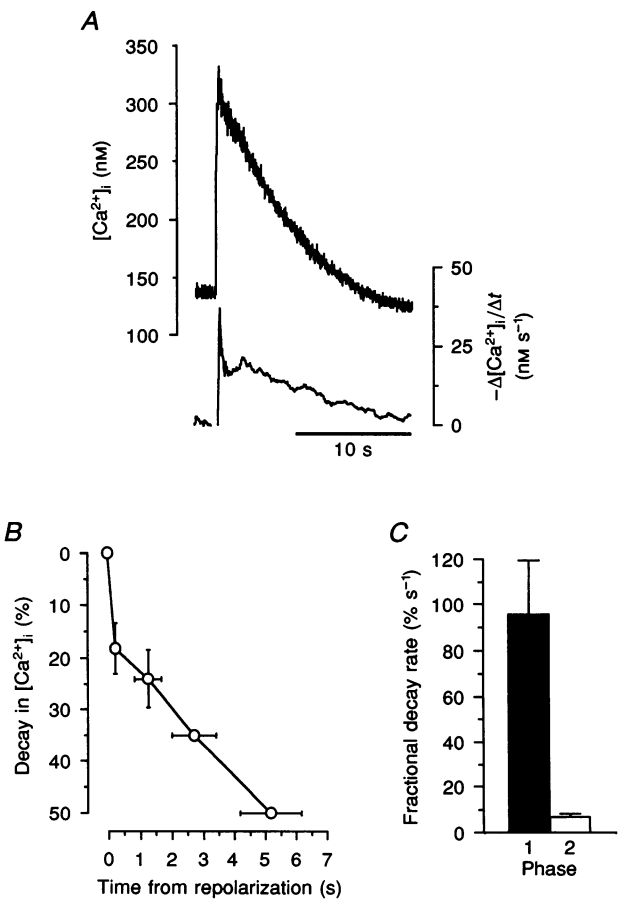

Figure 10. $[Ca^{2+}]_i$ decay in the presence of FCCP

A, $[Ca^{2+}]_i$ and $-\Delta[Ca^{2+}]_i/\Delta t$ records for a single cell exposed to 1 μM FCCP in the pipette solution and depolarized to +10 mV for 300 ms. *B*, summary of the decline in percentage $[Ca^{2+}]_i$ (means ± S.E.M.) for 6 cells (3 animals) treated with 1 μM FCCP. Note that the time axis has been compressed in comparison with other similar graphs. *C*, mean fractional rate of $[Ca^{2+}]_i$ decay (± S.E.M.) for the initial phase of rapid decline (phase 1) and from the end of phase 1 to 50% decay (phase 2).

Similar results were obtained when the protonophore FCCP was added to both bath and pipette solutions at a concentration of 1 μM. This agent also depolarizes the mitochondria but acts by increasing mitochondrial permeability to protons (Drummond & Fay, 1996). The secondary acceleration was blunted or absent in the presence of FCCP (Fig. 10*A*). In a series of six cells, an initial period of rapid decline in $[Ca^{2+}]_i$ was followed by a linear decay in percentage $[Ca^{2+}]_i$ to 50% (Fig. 10*B*), with no statistically significant increase in the rate of fall (Fig. 10*C*). Overall, the rate of decline after phase 1 was slower in the presence of 1 μM FCCP than with 2 mM CN^- or control solutions, as indicated by the increased time required for $[Ca^{2+}]_i$ to decay by 50% (Fig. 10*B*).

Both CN^- and FCCP might be expected to inhibit ATP production by mitochondria as well as blocking Ca^{2+} uptake. Although ATP was included in the pipette solution, it might be argued that the effects of these agents on the profile of $[Ca^{2+}]_i$ decline was secondary to reduced activity in Ca^{2+}-ATPases in the plasma membrane or sarcoplasmic reticulum. In an attempt to circumvent this objection, experiments were carried out in which 30 μM Ruthenium Red was included in the pipette solution. This should block Ca^{2+} uptake by the mitochondrial uniporter (Rossi, Vasington & Carafoli, 1973) without affecting ATP synthesis (Denton & McCormack, 1990). Like CN^- and FCCP, Ruthenium Red prevented the late acceleration of $[Ca^{2+}]_i$ decline seen under control conditions (Fig. 11*A*). The initial decay during phase 1 was still rapid, however, and accounted on average for 23 ± 4% of the total decline at a mean fractional decay rate of 133 ± 32% s^{-1} in five cells (Fig. 11*C*). The rate of fall then slowed considerably, with linear decline between the end of phase 1 and 50% decay at a mean rate of 17 ± 2% s^{-1} ($P < 0{\cdot}05$, Wilcoxon signed rank test; $n = 5$; Fig. 11*B* and *C*). These findings are consistent with the hypothesis that upregulation of mitochondrial Ca^{2+} uptake accounts for the secondary increase in the rate of $[Ca^{2+}]_i$ decay seen in many transients.

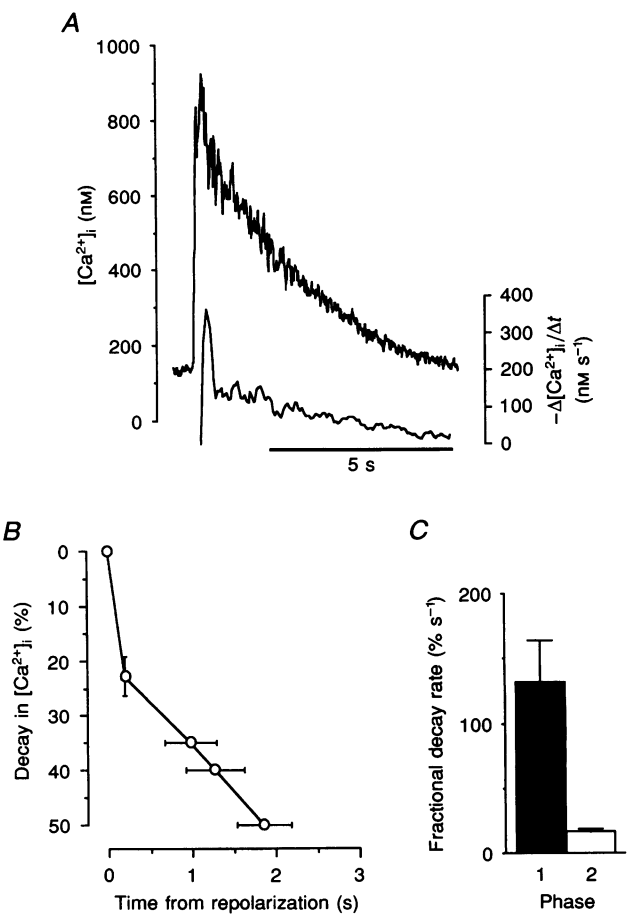

Figure 11. $[Ca^{2+}]_i$ decay in the presence of Ruthenium Red

A, $[Ca^{2+}]_i$ and $-\Delta[Ca^{2+}]_i/\Delta t$ records for a single cell exposed to 30 μM Ruthenium Red in the pipette solution and depolarized to +10 mV for 300 ms. *B*, summarized data (means ± S.E.M.) showing the decline in percentage $[Ca^{2+}]_i$ for 5 cells (1 animal) treated with 30 μM Ruthenium Red. *C*, mean fractional rate of $[Ca^{2+}]_i$ decay (± S.E.M.) for the initial phase of rapid decline (phase 1) and from the end of phase 1 to 50% decay (phase 2).

DISCUSSION

These experiments have revealed previously unreported complexities in the temporal profile of $[Ca^{2+}]_i$ decay in isolated smooth muscle cells. Under voltage clamp conditions, up to three distinct phases of decline were seen, with a quick-slow-quick pattern of $[Ca^{2+}]_i$ removal at both −110 mV and the more physiological potential of −50 mV (Figs 1–3). These phases differ in their dependence on time and $[Ca^{2+}]_i$, and different removal mechanisms appear to dominate during each.

Initial rapid $[Ca^{2+}]_i$ decline

The initial period of rapid decline in these experiments (phase 1; Fig. 1) was effectively time limited, i.e. it became shorter as the depolarizing pulse length increased and had a maximum duration of less than 1 s from the onset of depolarization (Figs 4 and 5). Such a phase of accelerated $[Ca^{2+}]_i$ decay may be accounted for if it is assumed that the rapid influx of Ca^{2+} during cell depolarization produces a high subsarcolemmal $[Ca^{2+}]$ and that this favours rapid Ca^{2+} removal. The latter assumption seems reasonable given the presence of a variety of Ca^{2+} removal systems adjacent to the subsarcolemmal space, including Na^+–Ca^{2+} exchangers (McCarron *et al.* 1994), Ca^{2+}-ATPase pumps in both the plasma membrane itself and in the near-membrane sarcoplasmic reticulum (see review by Missiaen *et al.* 1992), and mitochondria (Drummond & Fay, 1996). If the $[Ca^{2+}]$ in the region of these removal systems is disproportionately high immediately following depolarization, then the rate of Ca^{2+} efflux from the cytoplasm is likely to be higher than when the same total Ca^{2+} load is distributed evenly throughout the cell.

A variety of studies support the premise that cytoplasmic Ca^{2+} is not homogeneously distributed following activation of Ca^{2+} entry or release in vascular smooth muscle (Rembold *et al.* 1995), with unusually high $[Ca^{2+}]$ immediately beneath the plasma membrane being a likely cause of this non-uniformity (Stehno-Bittel & Sturek, 1992; Ganitkevich & Isenberg, 1996). Recent experiments using membrane-bound Ca^{2+} indicators have shown that the subsarcolemmal $[Ca^{2+}]$ rises faster and to higher levels than global $[Ca^{2+}]_i$ in *Bufo marinus* gastric myocytes depolarized from −80 to 0 mV (Etter *et al.* 1994, 1996). This intracellular gradient is short-lived, however, with the near-membrane $[Ca^{2+}]$ declining back towards the global $[Ca^{2+}]$ (measured with fura-2) during the latter part of a sustained depolarization (Etter *et al.* 1996). Presumably this is a consequence of inactivation of the inward Ca^{2+} flux through voltage-activated channels in the membrane and diffusion of Ca^{2+} into the body of the cell. Calculations based on near-membrane Ca^{2+} indicator measurements suggest that the subsarcolemmal $[Ca^{2+}]$ drops to a value similar to the global cytoplasmic concentration value about 400–500 ms after the onset of depolarization (Etter *et al.* 1996). Mathematical simulations of depolarization in these cells also predict that the $[Ca^{2+}]$ near the plasma membrane will be higher than that elsewhere for several hundreds of milliseconds (Kargacin & Fay, 1991; Kargacin, 1994). These predictions still apply if the only restriction placed on Ca^{2+} diffusion is a uniform reduction in diffusion coefficient throughout the cytoplasm, as observed experimentally (Allbritton, Meyer & Stryer, 1992). This could be amplified by the presence of a subsarcolemmal diffusion barrier (see Fig. 2*A* of Kargacin, 1994), perhaps in the form of the superficial layer of sarcoplasmic reticulum which has been identified in these cells (Moore *et al.* 1993). Whatever mechanism inhibits Ca^{2+} diffusion away from the sarcolemma, both the observed and predicted time courses of the intracellular $[Ca^{2+}]$ gradients are consistent with the observed time dependence of the rapid removal phase in the current experiments. For example, if we assume that the relevant removal processes are activated almost immediately after depolarization, which seems likely given the rapid onset of Ca^{2+} influx through voltage-operated channels, then the total duration of this phase was 456 ± 21 ms for 300 ms pulses under control conditions (i.e. phase 1 duration as measured from repolarization plus 300 ms; $n = 19$; Fig. 2). The more even distribution of intracellular $[Ca^{2+}]$ and lower subsarcolemmal $[Ca^{2+}]$ expected after longer pulses would also explain why no rapid phase of removal was seen using depolarizations of 1 s duration or longer (Fig. 4).

Although our results are in good agreement with the Ca^{2+} distribution model described above, a number of other factors should be considered. First, saturation of subsarcolemmal fura-2 by very high $[Ca^{2+}]$ may distort the recorded transients. Although such saturation may occur, however, redistribution of the Ca^{2+} load throughout the rest of the cytoplasm would be expected to produce an increase, rather than a decrease in the average fura-2 ratio for the cell, and so would tend to slow, rather than accelerate the apparent rate of $[Ca^{2+}]$ decay. Alternatively, one could postulate that a capacity-limited Ca^{2+} removal or slow buffer system, which becomes fully saturated about 500 ms after depolarization, might explain the time dependence seen. This seems unlikely, however, since changing the Ca^{2+} load by changing the test voltage had little effect on the early decline in $[Ca^{2+}]_i$ (Fig. 6). Finally, it might be argued that there is no change in the effective rate of Ca^{2+} removal during the transient but that $[Ca^{2+}]_i$ decay is slowed after about 500 ms by the delayed onset of an influx of Ca^{2+} into the cytoplasm. One candidate would be Ca^{2+}-induced Ca^{2+} release, triggered by high $[Ca^{2+}]_i$ (Iino, 1989). The reduction in the amplitude of transients recorded in the presence of ryanodine suggests that this process may contribute to the $[Ca^{2+}]_i$ rise during depolarization, as it does in some other smooth muscle cells (Ganitkevich & Isenberg, 1994). The failure of ryanodine and caffeine to alter the temporal profile of decay following repolarization, however, implies that Ca^{2+}-induced Ca^{2+} release does not explain the multiphasic decline seen (Fig. 7).

It seems reasonable to propose, therefore, that the initial rapid phase of decay reflects a period of preferential Ca^{2+} supply to the peripherally located removal mechanisms. Na^+–Ca^{2+} exchange appears to be particularly important during this phase since the initial fractional decay rate was reduced, on average, by 75% when extracellular Na^+ was removed (Fig. 8). The contribution of Na^+–Ca^{2+} exchange to early $[Ca^{2+}]_i$ decay following short depolarizations is consistent with its proposed role as a high-capacity but low-affinity Ca^{2+} removal system (Matlib, Kihgara, Farrell & Dage, 1988; Hilgemann, Nicoll & Philipson, 1991). Such a removal system might be expected to play a dominant role when the local (i.e. subsarcolemmal) $[Ca^{2+}]$ is unusually high. The voltage sensitivity of Na^+–Ca^{2+} exchange favours increased Ca^{2+} efflux at the negative membrane potentials used in the majority of these experiments (McCarron *et al.* 1994), but an initial phase of rapid decay was still seen following repolarization to −50 mV (Fig. 3). This suggests that, following a brief depolarization, the high subsarcolemmal $[Ca^{2+}]$ raises the reversal potential for Na^+–Ca^{2+} above −50 mV.

Secondary acceleration in $[Ca^{2+}]_i$ decay

A secondary increase in the rate of $[Ca^{2+}]_i$ decline (phase 3) was seen under control conditions providing peak $[Ca^{2+}]_i$ reached an adequate level (Figs 1 and 2). This was unaffected by repolarizing to −50 mV instead of to −110 mV (Fig. 3) but no such acceleration was seen when the test voltage was adjusted to produce a small rise in global $[Ca^{2+}]_i$ (Fig. 6), or following short (100 ms) pulses (Fig. 5). Both of these effects may be explained by a Ca^{2+}-dependent enhancement of Ca^{2+} removal since the peak global $[Ca^{2+}]_i$ achieved also increased with pulse duration (Fig. 4). For example, 100 ms pulses produced a mean rise in $[Ca^{2+}]_i$ of 315 ± 72 nM, compared with 473 ± 135 nM during 500 ms depolarizations ($P < 0{\cdot}02$, Wilcoxon signed rank test; $n = 8$). Ca^{2+}-dependent and persistent enhancement of Ca^{2+} removal has previously been described following depolarizing trains in these cells (Becker *et al.* 1989). The present study, however, provides the first evidence that such a mechanism may play a role in shaping $[Ca^{2+}]_i$ decay following single depolarizations similar in length to the recorded action potential (Walsh & Singer, 1987; Becker *et al.* 1989). The time course of the resulting transients suggests that enhancement of removal develops between 1·5 and 2 s after the rise in $[Ca^{2+}]_i$ (Figs 1 and 2). This is consistent with previous experiments using trains of pulses which demonstrated appreciable acceleration of $[Ca^{2+}]_i$ decay when trains lasting 2 s or longer were compared with single pulses (P. L. Becker, F. S. Fay, J. J. Singer & J. V. Walsh, unpublished data).

Several experiments were carried out to identify the removal mechanism responsible for this Ca^{2+}-dependent acceleration of $[Ca^{2+}]_i$ decay. Neither ryanodine nor caffeine blocked this phase (Fig. 7), suggesting that the increased slope is not due to the termination of Ca^{2+}-induced Ca^{2+} release. Again, delayed enhancement of removal was still observed when external Na^+ had been removed (Fig. 8), so it is unlikely that upregulation of Na^+–Ca^{2+} exchange is responsible. Inhibition of Ca^{2+} uptake by mitochondria, however, effectively prevented acceleration of removal, regardless of whether the electron transport chain was blocked using CN^- (Fig. 9), or the mitochondrial proton gradient was reduced using FCCP (Fig. 10). Both these agents reduce the electrical gradient between the mitochondrial matrix and the cytoplasm, thereby diminishing the driving force for Ca^{2+} uptake (Drummond & Fay, 1996). It might, of course, be argued that CN^- and FCCP are acting indirectly by reducing the ATP supply to Ca^{2+}-ATPases. This possibility cannot be completely excluded but it should be remembered that 3·5 mM ATP was included in the pipette solution and that treated cells still contracted in response to depolarization, indicating that the ATP supply was adequate for myosin light chain phosphorylation, a reaction with a higher K_m for ATP (50 μM; Adelstein & Klee, 1981) than that of the ion pumps (< 2·5 μM; Carafoli, 1991). The fact that cell dialysis with Ruthenium Red also prevented the delayed increase in the rate of $[Ca^{2+}]_i$ fall (Fig. 11) adds empirical weight to these theoretical considerations since this agent inhibits the mitochondrial Ca^{2+} uniporter and is less likely to affect ATP production. These results suggest, therefore, that the secondary acceleration in $[Ca^{2+}]_i$ decay during a single transient is due to Ca^{2+}-dependent upregulation of Ca^{2+} removal into mitochondria. This is consistent with the ability of these mitochondrial inhibitors to block the increase in the rate of $[Ca^{2+}]_i$ decline normally seen after prolonged depolarizing trains (Drummond & Fay, 1996).

Summary of Ca^{2+} handling following transmembrane Ca^{2+} influx

Based on the multiphasic $[Ca^{2+}]_i$ decline observed in the current experiments, along with the apparent time and Ca^{2+} dependence of the different phases seen, we propose that Ca^{2+} handling in *Bufo marinus* gastric myocytes has the following characteristics.

(1) Cell depolarization leads to rapid influx of Ca^{2+} across the plasma membrane, producing high levels of subsarcolemmal $[Ca^{2+}]$ adjacent to the major removal systems, of which Na^+–Ca^{2+} exchange is initially the most important at −110 mV. This produces rapid $[Ca^{2+}]_i$ removal, which is seen as an initial, relatively brief period of rapid $[Ca^{2+}]_i$ decline when the cell is repolarized after a short depolarization. With maintained depolarization, the influx is slowed due to inactivation of the current, and diffusion leads to a redistribution of the total cell Ca^{2+} load away from these areas and the decay rate of global $[Ca^{2+}]_i$ slows. Because of this the initial rapid phase of decline is not seen following prolonged depolarizations.

(2) There is a Ca^{2+}-dependent upregulation of Ca^{2+} removal which has relatively slow onset kinetics (approximately 2 s). This effect is dependent on Ca^{2+} uptake by mitochondria and leads to an acceleration of the rate of removal which is dependent on maintenance of an adequate $[Ca^{2+}]_i$ for an adequate time (it is not seen following short depolarizing

pulses or when the overall rise in $[Ca^{2+}]_i$ is small). The delay in onset suggests a multistep signal pathway, but the actual transduction mechanisms involved in this upregulation remain to be determined.

ADELSTEIN, R. S. & KLEE, C. B. (1981). Purification and characterization of smooth-muscle myosin light chain kinase. *Journal of Biological Chemistry* **256**, 7501–7509.

ALLBRITTON, N. L., MEYER, T. & STRYER, L. T. I. (1992). Range of messenger action of calcium ion and inositol 1,4,5-trisphosphate. *Science* **258**, 1812–1815.

BECKER, P. L., SINGER, J. J., WALSH, J. V. JR & FAY, F. S. (1989). Regulation of calcium concentration in voltage clamped smooth muscle cells. *Science* **244**, 211–214.

CARAFOLI, E. (1991). Calcium pump of the plasma membrane. *Physiological Reviews* **71**, 129–153.

CHEN, Q., CANNELL, M. & VAN BREEMEN, C. (1992). The superficial buffer barrier in vascular smooth muscle. *Canadian Journal of Physiology and Pharmacology* **70**, 509–514.

DANIEL, E. E., VAN BREEMEN, C., SCHILLING, W. P. & KWAN, C. Y. (1995). Regulation of vascular tone – crosstalk between sarcoplasmic reticulum and sarcolemma. *Canadian Journal of Physiology and Pharmacology* **73**, 551–557.

DENTON, R. M. & MCCORMACK, J. G. (1990). Ca^{2+} as a second messenger within mitochondria of the heart and other tissues. *Annual Review of Physiology* **52**, 451–466.

DRUMMOND, R. M. & FAY, F. S. (1996). Mitochondria contribute to Ca^{2+} removal in smooth muscle cells. *Pflügers Archiv* **431**, 473–482.

ETTER, E. F., KUHN, M. A. & FAY, F. S. (1994). Detection of changes in near-membrane Ca^{2+} concentration using a novel membrane-associated Ca^{2+} indicator. *Journal of Biological Chemistry* **269**, 10141–10149.

ETTER, E. F., MINTA, A., POENIE, P. & FAY, F. S. (1996). Near-membrane $[Ca^{2+}]$ transients resolved using the Ca^{2+} indicator, FFP18. *Proceedings of the National Academy of Sciences of the USA* **93**, 5368–5373.

FAY, F. S., HOFFMAN, R., LECLAIR, S. & MERRIAM, P. (1982). Preparation of individual smooth-muscle cells from the stomach of *Bufo marinus*. *Methods in Enzymology* **85**, 284–292.

GANITKEVICH, V. YA. & ISENBERG, G. (1994). Efficacy of peak Ca^{2+} currents (I_{Ca}) as trigger of sarcoplasmic reticulum Ca^{2+} release in myocytes from the guinea-pig coronary artery. *Journal of Physiology* **484**, 287–306.

GANITKEVICH, V. YA. & ISENBERG, G. (1996). Dissociation of subsarcolemmal from global cytosolic $[Ca^{2+}]$ in myocytes from guinea-pig coronary artery. *Journal of Physiology* **490**, 305–318.

GRYNKIEWICZ, A. M., POENIE, M. & TSIEN, R. Y. (1985). A new generation of Ca^{2+} indicators with greatly imporoved fluorescence properties. *Journal of Biological Chemistry* **260**, 3440–3450.

GUNTER, T. E. & PFEIFFER, D. R. (1990). Mechanisms by which mitochondria transport calcium. *American Journal of Physiology* **258**, C755–786.

GURNEY, A. M., TSIEN, R. Y. & LESTER, H. A. (1987). Activation of a potassium current by rapid photochemically generated step increases of intracellular calcium in rat sympathetic neurons. *Proceedings of the National Academy of Sciences of the USA* **84**, 3496–3500.

HILGEMANN, D. W., NICOLL, D. A. & PHILIPSON, K. D. (1991). Charge movement during Na^+ translocation by the native and cloned Na^+/Ca^{2+} exchanger. *Nature* **352**, 715–721.

IINO, M. (1989). Calcium-induced calcium release mechanism in guinea pig taenia caeci. *Journal of General Physiology* **94**, 363–383.

KARGACIN, G. (1994). Calcium signaling in restricted diffusion spaces. *Biophysical Journal* **67**, 262–272.

KARGACIN, G. & FAY, F. S. (1991). Ca^{2+} movement in smooth muscle cells studied with one- and two-dimensional diffusion models. *Biophysical Journal* **60**, 1088–1100.

KOSTYUK, P. G. & SHIROKOV, R. E. (1989). Deactivation kinetics of different components of calcium inward current in the membrane of mice sensory neurones. *Journal of Physiology* **409**, 343–355.

MCCARRON, J. G., MCGEOWN, J. G., REARDON, S., IKEBE, M., FAY, F. S. & WALSH, J. V. JR (1992). Calcium-dependent enhancement of calcium current in smooth muscle by calmodulin-dependent protein kinase II. *Nature* **357**, 74–77.

MCCARRON, J. G., WALSH, J. V. JR & FAY, F. S. (1994). Sodium/calcium exchange regulates cytoplasmic calcium in smooth muscle. *Pflügers Archiv* **426**, 199–205.

MCGEOWN, J. G. & FAY, F. S. (1995). Calcium decline following short depolarizations is multiphasic in isolated gastric myocytes from *Bufo marinus*. *Journal of Physiology* **489.P**, 135*P*.

MCGEOWN, J. G., MCCARRON, J. G., DRUMMOND, R. M. & FAY, F. S. (1996). Identification of removal mechanisms shaping the temporal profile of calcium decay in gastric myocytes from *Bufo marinus*. *Irish Journal of Medical Science* (in the Press).

MATLIB, M. A., KIHARA, M., FARRELL, C. & DAGE, R. C. (1988). The Na^+–Ca^{2+} exchange in vascular smooth muscle cell membrane vesicles from culture cells and from tissue is similar. *Biochimica et Biophysica Acta* **939**, 173–177.

MISSIAEN, L., DESMEDT, H., DROOGMANS, G., HIMPENS, B. & CASTEELS, R. (1992). Calcium-ion homeostasis in smooth-muscle. *Pharmacology and Therapeutics* **56**, 191–231.

MOORE, E. D. W., ETTER, E. F., PHILIPSON, K. D., CARRINGTON, W. A., FOGARTY, K. E., LIFSHITZ, L. M. & FAY, F. S. (1993). Coupling of the Na^+/Ca^{2+} exchanger, Na^+/K^+ pump and sarcoplasmic reticulum in smooth muscle. *Nature* **365**, 657–660.

MOREL, N. & GODFRAIND, T. (1984). Sodium calcium exchange in smooth-muscle microsomal fractions. *Biochemical Journal* **218**, 421–427.

REMBOLD, C. M., VAN RIPER, D. A. & CHEN, X.-L. (1995). Focal $[Ca^{2+}]_i$ increases detected by aequorin but not by fura-2 in histamine- and caffeine-stimulated swine carotid artery. *Journal of Physiology* **488**, 549–564.

ROSSI, C. S., VASINGTON, F. D. & CARAFOLI, E. (1973). The effect of ruthenium red on the uptake and release of Ca^{2+} by mitochondria. *Biochemical and Biophysical Research Communications* **50**, 846–852.

SCHEID, C. R. & FAY, F. S. (1984). Transmembrane ^{45}Ca fluxes in isolated smooth muscle cells: basal Ca^{2+} fluxes. *American Journal of Physiology* **246**, C422–430.

SINGER, J. J. & WALSH, J. V. JR (1987). Characterization of calcium-activated potassium channels in single smooth muscle cells using the patch-clamp technique. *Pflügers Archiv* **408**, 98–111.

SOMLYO, A. P. (1985). Excitation–contraction coupling and the ultrastructure of smooth muscle. *Circulation Research* **57**, 497–507.

STEHNO-BITTEL, L. & STUREK, M. (1992). Spontaneous sarcoplasmic reticulum calcium release and extrusion from bovine, not porcine, coronary artery smooth muscle. *Journal of Physiology* **451**, 49–78.

TSIEN, R. W. & TSIEN, R. Y. (1990). Calcium channels, stores and oscillations. *Annual Review of Cell Biology* **6**, 715–760.

VAN BREEMEN, C. & SAIDA, K. (1989). Cellular mechanisms regulating $[Ca^{2+}]_i$ in smooth muscle. *Annual Review of Physiology* **51**, 315–329.

WALSH, J. V. JR & SINGER, J. J. (1987). Identification and characterization of major ionic currents in isolated smooth muscle cells using the voltage-clamp technique. *Pflügers Archiv* **408**, 83–97.

WILLIAMS, D. A., FOGARTY, K. E., TSIEN, R. Y. & FAY, F. S. (1985). Calcium gradients in single smooth-muscle cells revealed by the digital imaging microscope using fura-2. *Nature* **318**, 558–561.

YAGI, S., BECKER, P. L. & FAY, F. S. (1988). Relationship between force and Ca^{2+} concentration in smooth muscle as revealed by measurements on single cells. *Proceedings of the National Academy of Sciences of the USA* **85**, 4109–4113.

Acknowledgements

This work was supported by grants from The Wellcome Trust (grant no. 038710/Z/93/Z to J.G.McG. and grant no. 036885/Z/92/Z to J.G.McC.) and NIH (HL14523 and HL47530 to F.S.F.), and a postdoctoral fellowship from the Massachusetts Heart Association (R.M.D.). We wish to thank Kristine Perry and Jeff Carmichael for their expert technical assistance.

Author's email address

F. S. Fay: fsf@invivo.ummed.edu

Received 22 May 1996; accepted 17 September 1996.